Journal of Coordination Chemistry
Publication details, including instructions for authors and subscription information:
http://www.tandfonline.com/loi/gcoo20

Synthesis, DNA-binding, and photocleavage properties of Ru(II) complexes containing dppz-based ligand

Xue-Wen Liu [a a b], Yuan-Dao Chen [a b] & Lin Li [a]

[a] College of Chemistry and Chemical Engineering, Hunan University of Arts and Science, ChangDe 415000, P.R. China

[b] Key Lab of Environment-Friendly Chemistry and Application in Ministry of Education, Xiangtan University, Xiangtan 411105, P.R. China

Accepted author version posted online: 10 Jul 2012.Published online: 20 Jul 2012.

To cite this article: Xue-Wen Liu, Yuan-Dao Chen & Lin Li (2012) Synthesis, DNA-binding, and photocleavage properties of Ru(II) complexes containing dppz-based ligand, Journal of Coordination Chemistry, 65:17, 3050-3063, DOI: 10.1080/00958972.2012.710749

To link to this article: http://dx.doi.org/10.1080/00958972.2012.710749

Journal of Coordination Chemistry
Vol. 65, No. 17, 10 September 2012, 3050–3063

Synthesis, DNA-binding, and photocleavage properties of Ru(II) complexes containing dppz-based ligand

XUE-WEN LIU*†‡, YUAN-DAO CHEN†‡ and LIN LI†

†College of Chemistry and Chemical Engineering, Hunan University of Arts and Science, ChangDe 415000, P.R. China
‡Key Lab of Environment-Friendly Chemistry and Application in Ministry of Education, Xiangtan University, Xiangtan 411105, P.R. China

(*Received 5 January 2012; in final form 8 June 2012*)

A ligand ipdp (ipdp = indeno[1′,2′ : 5,6]pyrazino[2,3-i]dipyrido[3,2-*a* : 2′,3′-*c*]phenazine-8-one) and its ruthenium complexes, $[Ru(L)_2(ipdp)]^{2+}$ (L = bpy (2,2′-bipyridine), phen (1,10-phenanthroline)), have been synthesized and characterized by elemental analysis, electrospray mass spectra, and ^1H NMR. The interaction between the complexes and calf thymus DNA (CT-DNA) has been investigated by spectroscopic methods and viscosity measurements. The results indicate that the complexes can bind to CT-DNA in an intercalative mode. In addition, both complexes promote the photocleavage of plasmid pBR322 DNA under irradiation. The mechanistic studies reveal that singlet oxygen $^1O_2$ plays a significant role in DNA photocleavage.

Keywords: Ru(II) complex; dppz-based ligand; DNA-binding; Photocleavage

1. Introduction

Binding studies of small molecules to DNA are very important in their potential applications as chemical and stereoselective probes of nucleic acid structures, as molecular ''light switches'', and as anti-cancer drugs or complexes with other biological functions [1–8]. Small molecules can bind to DNA through three non-covalent modes, electrostatic binding, groove binding, or intercalation. Ru(II) complexes with polypyridyl ligands, due to their rich photochemical properties and a combination of rigid chiral structures spanning all three spatial dimensions, have been extensively applied to DNA-binding and DNA photocleavage. Many polypyridyl-type ligands (L) and their corresponding Ru(II) complexes $[Ru(phen)_2L]^{2+}$, $[Ru(bpy)_2L]^{2+}$ show interesting properties upon binding to DNA [9–13]. Of these, $[Ru(bpy)_2(dppz)]^{2+}$ (bpy = (2,2′-bipyridine); dppz = dipyrido[3,2-*a* : 2′,3′-*c*]phenazine) has been known as a molecular ''light switch'' for DNA, because it shows negligible background emission in aqueous solution at ambient temperature but displays strong luminescence after binding to DNA by intercalation [7]. Although $[Ru(bpy)_2(dppz)]^{2+}$ and other

*Corresponding author. Email: liuxuewen050@sina.com

ISSN 0095-8972 print/ISSN 1029-0389 online © 2012 Taylor & Francis
http://dx.doi.org/10.1080/00958972.2012.710749

Ru(II)-dppz systems exhibit strong DNA-binding affinity, they are poor singlet oxygen ($^1O_2$) sensitizers [14, 15], and their DNA-photocleavage efficiencies were rather low due to their short lifetime and low oxidizing ability in excited states [16]. Ru(II)-dppz systems improve their DNA-photocleavage properties mainly through modifications of the intercalating ligand dppz with photoreactive groups or polyazaaromatic units [17–22] or introduction of new ancillary ligands [14, 23]. Many reports have shown that Ru(II) polypyridyl complexes with modified dppz-based ligand have special DNA-binding, spectral, and DNA-photocleavage properties [17–22, 24–33]. Therefore, modification of the Ru(II)-dppz system is necessary for improving DNA-photocleavage properties of Ru(II)-dppz systems.

To gain more information on the DNA-binding properties of Ru(II) complexes and the influence of modified dppz for DNA-photocleavage properties, in this article, we report the synthesis and characterization of two ruthenium complexes containing modified dppz, $[Ru(L)_2(ipdp)]^{2+}$ (L = bpy (2,2′-bipyridine), phen (1,10-phenanthroline); ipdp = indeno[1′,2′ : 5,6]pyrazino[2,3-i]dipyrido[3,2-*a* : 2′,3′-*c*]phenazine-8-one).
Furthermore, the DNA-binding, DNA-photocleavage, and spectral properties of these Ru(II) complexes were investigated by electronic absorption, emission titration, competitive binding experiments, viscosity measurements, and photoactivated cleavage.

2. Experimental

2.1. *Materials and methods*

cis-$[Ru(bpy)_2Cl_2]\cdot 2H_2O$, *cis*-$[Ru(phen)_2Cl_2]\cdot 2H_2O$ [34] and 11,12-diaminodipyrido[3,2-*a* : 2′,3′-*c*]phenazine (dadppz) [35] were synthesized according to methods in the literature. Other materials were commercially available and used without purification. Supercoiled pBR322 DNA was purchased from MBI Fermentas. Calf thymus DNA (CT-DNA) was obtained from Sigma (St. Louis, MO, USA). Solutions of CT-DNA in buffer A gave a ratio of UV absorbance of 1.8–1.9 : 1 at 260 and 280 nm, indicating that the DNA was sufficiently free of protein [36]. The concentration of DNA per nucleotide was determined by absorption spectroscopy using the molar absorption coefficient ($6600\,(mol\,L^{-1})^{-1}\,cm^{-1}$) at 260 nm [37].

2.2. *Physical measurement*

C, H, and N element analyses were carried out with a Perkin-Elmer 240Q elemental analyzer. Fast atomic bombardment mass spectra (FAB-MS) were obtained on a VG ZAB-HS spectrometer. Electrospray mass spectra (ES-MS) were recorded using an LQC system (Finnigan MAT, USA) and the quoted m/z values are for the major peaks in the isotope distribution. ^1H NMR spectra were recorded on a Bruker ARX-500 spectrometer with $(CD_3)_2SO$ as solvent for the complexes at room temperature. Absorption spectra were recorded with a Shimadzu UV-2450 spectrophotometer and emission spectra on a Hitachi F-2500 spectrofluorophotometer at room temperature.

2.3. *DNA-binding experiments*

All DNA-binding experiments were carried out in buffer A (50 mmol L^{-1} NaCl, 5 mmol L^{-1} Tris–HCl, pH = 7.2). For DNA-photocleavage experiments, Ru(II) complexes and DNA samples were treated in buffer B (50 mmol L^{-1} Tris, 18 mmol L^{-1} NaCl, pH = 7.8). Electrophoresis experiments were carried out in TBE buffer C (89 mmol L^{-1} Tris-boric acid, 2 mmol L^{-1} EDTA, pH = 8.3).

Absorption titrations of Ru(II) complexes in buffer A were carried out at room temperature to determine the DNA-binding affinities between complex and DNA. During the titrations, fixed ruthenium complex concentration (20 μ mol L^{-1}) was employed and ruthenium-DNA solutions were allowed to incubate for 5 min before the absorption spectra were recorded. The intrinsic binding constants K of the complexes to DNA were calculated by a non-linear least-squares method according to equation (1) [38],

$$(\varepsilon_a - \varepsilon_f)/(\varepsilon_b - \varepsilon_f) = \left(b - \left(b^2 - 2K^2C_t[\mathrm{DNA}]/s\right)^{1/2}\right)/2KC_t, \tag{1a}$$

$$b = 1 + KC_t + K[\mathrm{DNA}]/2s, \tag{1b}$$

where [DNA] is the concentration of DNA in M (nucleotide), ε_a is the extinction coefficient observed for the ^{1}MLCT absorption at a given DNA concentration, ε_f is the extinction coefficient of the free complex without DNA, and ε_b is the extinction coefficient of the complex fully bound to DNA. K is the equilibrium binding constant in M^{-1}, C_t is the total metal complex concentration, and s is the binding site size.

For competitive binding experiments, emission spectra were recorded from 530 to 750 nm using Ru(II) complex as quencher, and sample was excited at 515 nm. Fluorescence quenching studies were conducted by adding increasing amounts of Ru(II) complexes directly into the samples containing 5 μmol L^{-1} ethidium bromide (EB) and 80 μmol L^{-1} DNA in buffer A.

DNA viscosities were measured using an Ubbelohde viscometer maintained at 30.0 ± 0.1°C in a thermostatic bath. DNA samples for viscosity measurement were prepared by sonication in order to minimize complexities arising from DNA flexibility. Every sample was measured at least three times and an average flow time was calculated. Data are presented as $(\eta/\eta_0)^{1/3}$ *versus* binding ratio [39], where η is the viscosity of DNA in the presence of complex and η_0 is the viscosity of DNA alone. The DNA viscosity values were calculated according to $\eta = (t - t_0)/t_0$, where t is the flow time of the solutions and t_0 is the flow time of buffer alone.

2.4. *DNA-photocleavage experiment*

DNA photocleavage by Ru(II) complexes was measured by the conversion of supercoiled pBR322 plasmid DNA to nicked circular and linear DNA forms. Supercoiled pBR322 DNA (0.1 μg) was treated with different concentrations of Ru(II) complexes in buffer B, and the solutions were incubated for 1 h in the dark, then irradiated at room temperature with an UV lamp (365 nm, 10 W). The samples were analyzed by electrophoresis for 2 h at 75 V on a 1% agarose gel in TBE buffer C. The gel was stained with 1 μg mL^{-1} EB and then photographed under UV light.

2.5. *Quantum yield of $^1O_2$ generation*

The reaction of $^1O_2$ with 1,3-diphenylisobenzofuran (DPBF) is utilized to quantitatively measure the $^1O_2$ generation quantum yields of Ru(II) complexes [23, 40, 41]. Air-saturated methanol solutions (2 mL) containing DPBF (0.1 μmol L^{-1}) and complexes (0.5 μmol L^{-1}) were placed in a 1 cm path fluorescence cuvette and illuminated with light of 450 nm (obtained from Hitachi F-2500 spectrofluorophotometer, 5 nm excitation slit width). The consumption of DPBF was followed by monitoring the decrease in fluorescence intensity of DPBF at the emission maximum ($\lambda_{ex} = 405$ nm, $\lambda_{em} = 479$ nm) at different irradiation times.

The $^1O_2$ generation quantum yield (Φ_Δ) was calculated according to equation (2), where I_{in} is the incident monochromatic light intensity, Φ_{ab} is the light absorbing efficiency of the photosensitizer, Φ_r is the reaction quantum yield of $^1O_2$ with DPBF, t is the irradiation time, I_0 and I_t are the fluorescence intensities of DPBF before and after irradiation, k is the slope, and superscript s stands for standard.

$$\frac{-\Delta[\mathrm{DPBF}]}{t} = \frac{I_0 - I_t}{t} = I_{in}\Phi_{ab}\Phi_\Delta\Phi_r \tag{2a}$$

$$\frac{k}{k^s} = \frac{\Phi_{ab}}{\Phi_{ab}^s} = \frac{\Phi_\Delta}{\Phi_\Delta^s} \tag{2b}$$

2.6. *Synthesis*

2.6.1. Indeno[1′,2′ : 5,6]pyrazino[2,3-i]dipyrido[3,2-a : 2′,3′-c]phenazine-8-one (ipdp). A solution of 11,12-diamino-dipyrido[3,2-*a* : 2′,3′-*c*]phenazine (dadppz) (0.093 g, 0.3 mmol) and ninhydrin (0.054 g, 0.3 mmol) in 5% dilute acetic acid (60 mL) was stirred for 2 h at room temperature. The dark brown precipitate was collected by filtration, washed with water, and vacuum-dried. Yield: 0.094 g, 71.8%. Anal (%) (Found: C, 74.45; H, 2.81; N, 19.04. Calcd for $C_{27}H_{12}N_6O$: C, 74.29; H, 2.77; N, 19.27). FAB-MS: $m/z = 437$ ($[M + 1]^+$).

2.6.2. $[Ru(bpy)_2(ipdp)](ClO_4)_2$ (1). A mixture of ipdp 0.120 g (*ca* 0.3 mmol), $[Ru(bpy)_2Cl_2]\cdot 2H_2O$ (0.156 g, 0.3 mmol) and ethylene glycol (10 mL) was refluxed under argon for 4 h. Upon cooling, the resulting solution was diluted with water (*ca* 60 mL), then treated with a saturated aqueous solution of $NaClO_4$. The dark brown precipitate was collected and purified by column chromatography on neutral alumina with acetonitrile–toluene (2 : 1, v/v) as eluent. The main red band was collected. The solvent was removed under reduced pressure and red microcrystals were obtained. Yield: 0.165 g, 52.5%. Anal (%) (Found: C, 53.98; H, 2.61; N, 13.22. Calcd for $C_{47}H_{28}N_{10}O_9RuCl_2$: C, 53.83; H, 2.69; N, 13.36). ES-MS (CH_3CN): $m/z = 949.6$ ($[M - ClO_4^-]^+$), 425.2 ($[M - 2ClO_4^-]^{2+}$). ^1H NMR (500 MHz, ppm, DMSO-d_6): 9.62 (s, 2H), 8.91 (t, 5H, $J_1 = 9.0$ Hz, $J_2 = 11.0$ Hz), 8.26 (t, 4H, $J_1 = 7.5$ Hz, $J_2 = 8.0$ Hz), 8.18 (t, 3H, $J_1 = 7.5$ Hz, $J_2 = 8.0$ Hz), 8.06 (t, 3H, $J_1 = 6.0$ Hz, $J_2 = 6.0$ Hz), 7.86 (m, 6H), 7.63 (t, 3H, $J_1 = 6.5$ Hz, $J_2 = 6.5$ Hz), 7.45 (m, 2H).

2.6.3. [Ru(phen)$_2$(ipdp)](ClO$_4$)$_2$ (2). This red complex was obtained by a similar method to that as described for **1** with the only difference that [Ru(phen)$_2$]Cl$_2 \cdot 2$H$_2$O (0.170 mg, 0.3 mmol) was used instead of [Ru(bpy)$_2$]Cl$_2 \cdot 2$H$_2$O. Yield: 0.189 g, 57.6%. Anal (%) (Found: C, 55.94; H, 2.68; N, 12.51, Calcd for $C_{51}H_{28}N_{10}O_9RuCl_2$: C, 55.85; H, 2.57; N, 12.77). ES-MS (CH_3CN): $m/z = 997.6$ ($[M - ClO_4^-]^+$), 449.1 ($[M-2ClO_4^-]^{2+}$). ^{1}H NMR (500 MHz, ppm, DMSO-d$_6$): 9.63 (dd, 2H, $J_1 = 8.0$ Hz, $J_2 = 9.0$ Hz), 9.34 (s, 1H), 9.21 (s, 1H), 8.80 (dd, 4H, $J_1 = 8.5$ Hz, $J_2 = 7.5$ Hz), 8.42 (s, 4H), 8.32 (m, 3H), 8.22 (t, 2H, $J = 8.0$ Hz), 8.07 (d, 2H, $J = 5.0$ Hz), 8.02 (m, 2H), 7.94 (dd, 2H, $J_1 = 8.0$ Hz, $J_2 = 6.5$ Hz), 7.86 (m, 3H), 7.70 (dd, 2H, $J_1 = 5.5$ Hz, $J_2 = 3.0$ Hz).

3. Results and discussion

3.1. *Synthesis and characterization*

The syntheses of the ligand and its complexes are presented in scheme 1. The ligand was obtained by a method similar to that described by Ruhemann and Shapiro [42, 43]; condensation of ninhydrin with the precursor diamine compound (dadppz) in dilute acetic acid gave ipdp. Complexes **1** and **2** were obtained by direct reaction of ligand with the appropriate mole ratios of the precursor complexes in ethylene glycol. All these complexes were purified by column chromatography and characterized by elemental

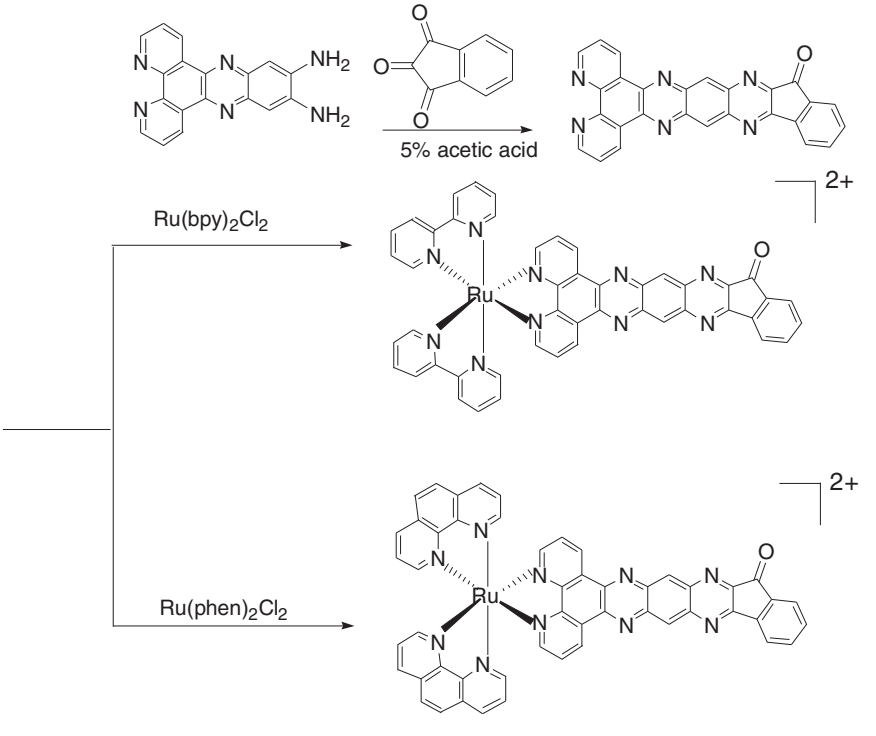

Scheme 1. The synthetic routes of ligand, $[Ru(bpy)_2(ipdp)]^{2+}$ and $Ru(phen)_2(ipdp)]^{2+}$.

analysis, ES-MS, and ^{1}H NMR. In the electrospray mass spectrometry for **1** and **2**, only the signals of $[M - ClO_4^-]^+$ and $[M - 2ClO_4^-]^{2+}$ were observed. In both cases, the doubly charged species was major peak. The measured molecular weights were consistent with expected values.

$[Ru(bpy)_2(ipdp)]^{2+}$ and $Ru(phen)_2(ipdp)]^{2+}$ gave well-defined ^{1}H NMR spectra (figure S1). The proton chemical shifts were assigned based on comparison with those of similar compounds [17, 20, 26–29]. The chemical shifts of all the protons in the aromatic region are presented in section 2.

3.2. *Electronic absorption titration*

The interaction of small molecules with DNA is characterized classically by absorption titration. Complex bound to DNA by intercalation usually results in change in absorbance (hypochromism) and red shift (bathochromism) because of intercalation involving a strong π–π stacking interaction between aromatic chromophore and the base pairs of DNA. The extent of hypochromism in the visible ^{1}MLCT band depends on intercalative binding strength [32].

Electronic absorption spectra of **1** and **2** in buffer A exhibited three well-resolved bands from 200–650 nm. The lowest energy bands at 443 nm for **1** and 442 nm for **2** are attributed to metal-to-ligand charge transfer (MLCT), bands in the range of 300–400 nm are assigned to intraligand π–π^* transitions, and the bands at 289 nm for **1** and 264 nm for **2** are assigned to bpy-centered π–π^* transitions and phen-centered π–π^* transitions in comparison with $[Ru(bpy)_3]^{2+}$ and $[Ru(phen)_3]^{2+}$, respectively. Absorption spectra of **1** and **2** in the absence and presence of CT-DNA (at a constant concentration of complexes, $[Ru] = 20\,\mu mol\,L^{-1}$) are shown in figure 1. With increasing concentration of DNA, both complexes show considerable decrease in absorptivity (hypochromism). For **1**, the hypochromism in the ^{1}MLCT band reaches as high as 24.4% at 443 nm at a ratio of [DNA]/[Ru] = 4.8. For **2**, upon addition of DNA, the MLCT band at 442 nm exhibits hypochromicity of 44.0% at a ratio of [DNA]/[Ru] = 3.6. Hypochromicity of Ru(II) complexes suggests that there are interaction between the complexes and DNA.

In order to compare quantitatively the DNA-binding strength, the changes of the ^{1}MLCT absorbance at 443 nm for **1** and at 442 nm for **2** were used to derive the intrinsic binding constants K of these two complexes bound to CT-DNA according to equation (1) [38]. The intrinsic binding constants K of the complexes were $7.9 \pm 0.4 \times 10^5\,(mol\,L^{-1})^{-1}$ ($s = 0.98$) for **1** and $2.1 \pm 0.7 \times 10^6\,(mol\,L^{-1})^{-1}$ ($s = 0.78$) for **2**. These values are compared to those of Ru(II) complexes with dppz-based ligands, $[Ru(bpy)_2(ppd)]^{2+}$ ($1.3 \times 10^6\,(mol\,L^{-1})^{-1}$) [20], $[Ru(phen)_2(hqdppz)]^{2+}$ ($(1 \pm 0.2) \times 10^5\,(mol\,L^{-1})^{-1}$), $[Ru(phen)_2(qdppz)]^{2+}$ ($> 10^6\,(mol\,L^{-1})^{-1}$) [39], $[Ru(phen)_2(ppn)]^{2+}$ ($2.6 \times 10^6\,(mol\,L^{-1})^{-1}$) [26], and $[Ru(bpy)_2(pp[2,3]p)]^{2+}$ ($6.9 \times 10^5\,(mol\,L^{-1})^{-1}$) [44], but smaller than that of $[Ru(phen)_2(dppz)]^{2+}$ ($5.1 \times 10^6\,(mol\,L^{-1})^{-1}$) [45]. In addition, **2** exhibits stronger DNA-binding affinity than **1**. As reported before, DNA-binding affinity of complexes can be influenced by the different plane area and hydrophobicity of the ancillary ligands [46, 47]. The greater DNA-binding affinity for **2** can be attributed to the ancillary ligand phen with greater plane area and hydrophobicity (relative to bpy). The experiment results suggest that the complexes bind to DNA with

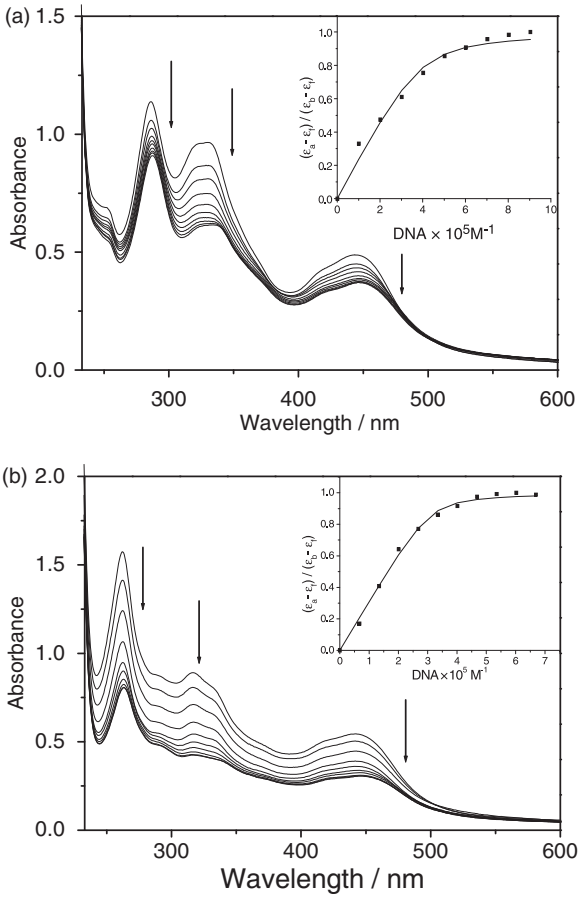

Figure 1. Absorption spectra of **1** (a) and **2** (b) in buffer A upon addition of CT-DNA, [Ru] = 20 μmol L^{-1}, [DNA] = 0 – 100 μmol L^{-1}. The arrow shows the absorbance changing upon increase in DNA concentration. Inset: plots of $(\varepsilon_a - \varepsilon_f)/(\varepsilon_b - \varepsilon_f)$ *vs*. [DNA] for the titration of DNA to Ru(II) complexes.

high DNA affinities. Further investigations are needed to elucidate the DNA-binding mode of the complexes.

3.3. *Emission spectra*

Emission spectroscopic studies give additional evidence for DNA-binding mode. Changes in luminescence spectra of the complexes in the presence of DNA in buffer A are shown in figure 2. In the absence of DNA, **1** and **2** show fluorescence in buffer solution. Upon the addition of aliquots of CT-DNA solutions to aqueous solutions of both complexes, emission intensities of **1** and **2** grow to *ca* 1.35 and 1.49 times and saturate at a [DNA]/[Ru] ratio of 22.5 for **1** and 17.5 for **2**. This implies that both Ru(II) complexes interact with CT-DNA and DNA protects them, since the hydrophobic environment inside the DNA helix reduces the accessibility of solvent water to the complex and the complex mobility is restricted at the binding site, leading to decreased vibration modes of relaxation.

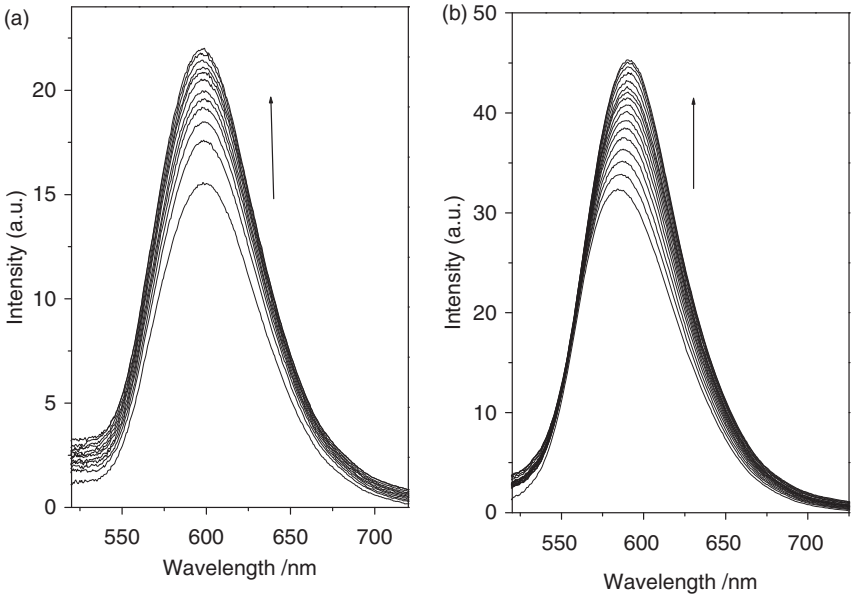

Figure 2. Emission spectra of Ru(II) complexes (5 μmol L^{-1}) **1** (a) and **2** (b) in buffer A at 298 K in the absence and presence of CT-DNA. The arrow shows the intensity change upon increase in DNA concentration.

Steady-state emission quenching experiments using $[Fe(CN)_6]^{4-}$ as quencher may provide more information about the interaction between the two complexes and DNA, although it cannot determine the DNA-binding mode of complex. As shown in figure 3, the emission quenching curves were in agreement with the linear Stern–Volmer equation. In the absence of DNA, the emissions of **1** and **2** were efficiently quenched by $[Fe(CN)_6]^{4-}$, and the Stern–Volmer constant K_{sv} value was derived to be 1.39 for **1** and 3.52 for **2**. However, in the presence of DNA, the emission of the two complexes were difficult to be quenched by $[Fe(CN)_6]^{4-}$, and the Stern–Volmer constant K_{sv} values of **1** and **2** were 0.85 and 0.78, respectively. Ru(II) complex cations are protected efficiently by DNA, due to repulsion of the highly negative $[Fe(CN)_6]^{4-}$ from the DNA polyanion backbone which hinders access of $[Fe(CN)_6]^{4-}$ to the DNA-bound complexes [48]. The curvature reflects different extent of protection of bound Ru(II) complex cations, a larger slope for the Stern–Volmer curve parallels poorer protection and lower binding. From figure 3, **2** binds to DNA more strongly than **1**.

3.4. *Competitive binding experiments*

Competitive binding experiments offer further information about the DNA-binding mode and the apparent DNA-binding constant from a well-established quenching assay based on displacement of the intercalating EB from CT-DNA. The molecular fluorophore EB can emit strong fluorescence in the presence of DNA due to strong intercalation between adjacent DNA base pairs. If the second molecule could not emit on excitation at a certain wavelength and could replace EB from DNA-bound EB, it results in sharp fluorescence quenching of the solutions as free EB shows no apparent

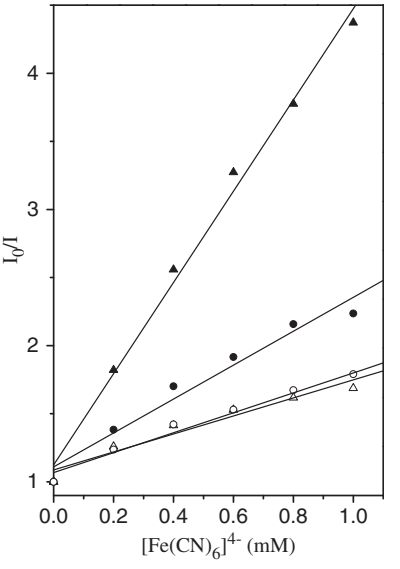

Figure 3. Emission quenching curves of **1** (•), **1** + DNA (○), **2** (▲), and **2** + DNA (△) with increasing concentration of $[Fe(CN)_6]^{4-}$. [Ru] = 5 μmol L^{-1}, [DNA]/[Ru] = 40.

emission intensity in buffer A. Free EB molecules were easily quenched by surrounding water [49]. On excitation at 515 nm, free EB, Ru(II) complexes, and DNA-bound Ru(II) complexes show negligible fluorescence, which does not influence the quenching experiment results. Figure 4 shows fluorescence quenching spectra of DNA-bound EB by Ru(II) complexes. Upon addition of Ru(II) complexes, sharp decreases were observed, indicating both complexes could displace EB from DNA. From data in figure 4, in the plot of percentage of quenching fluorescence, $(I_0 - I)/I_0$ *versus* [Ru]/[EB], 50% EB molecules were displaced from adjacent DNA base pairs at a concentration ratio of [Ru]/[EB] = 2.71 for **1** and 2.16 for **2**. By taking the DNA-binding constant of $1.4 \times 10^6 (\text{mol L}^{-1})^{-1}$ for EB [50, 51], the apparent DNA-binding constants K_{app} of the two complexes were calculated according to equation (3) [52],

$$K_{app} = K_{EB}([\text{EB}]_{50\%}/[\text{Ru}]_{50\%}) \tag{3}$$

where K_{app} is the apparent DNA-binding constant of the Ru(II) complex, K_{EB} is the DNA-binding constant of EB, and $[\text{EB}]_{50\%}$ and $[\text{Ru}]_{50\%}$ are the EB and Ru(II) complex concentrations at 50% fluorescence, respectively.

The values were $5.17 \times 10^5 (\text{mol L}^{-1})^{-1}$ for **1** and $6.48 \times 10^5 (\text{mol L}^{-1})^{-1}$ for **2**, respectively, which is slightly smaller than the intrinsic binding constant K values derived from absorption titration data. In addition, the fluorescence of EB bound to DNA was nearly completely quenched at a concentration ratio of [Ru]/[EB] = 12.40 for **1** and 9.23 for **2**, confirming that **2** exhibits greater DNA-binding affinity than **1**.

3.5. *Viscosity properties*

To further clarify the DNA-binding properties and the binding mode of **1** and **2**, the viscosity measurements were carried out on CT-DNA by varying the concentration

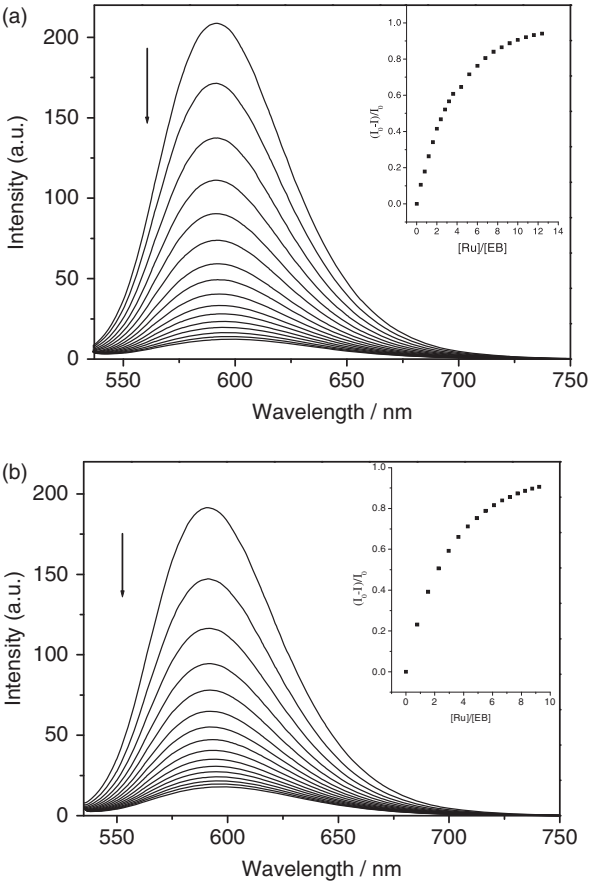

Figure 4. Fluorescence quenching spectra of EB bound to DNA by **1** (a) and **2** (b), [DNA] = 80 μmol L^{-1}, [EB] = 5 μmol L^{-1}. The arrow shows the intensity change upon increasing Ru(II) complexes concentration. Inset: plots of relative integrated fluorescence intensity *vs.* [Ru]/[EB].

of added complex. It is well known that DNA viscosity measurement is a useful means of determining whether a complex intercalates into DNA. Classical intercalative binding would cause elongation of the DNA helix as base pairs are separated to accommodate the bound ligand, resulting in increase of DNA viscosity. In contrast, a partial, non-classical intercalation of the ligand could bend (or kink) the DNA helix, resulting in decrease of DNA viscosity [53–55]. Electrostatic binding has little effect on DNA viscosity.

The changes in DNA viscosity upon addition of EB, **1**, **2**, and $[Ru(bpy)_3]^{2+}$ are shown in figure 5. $[Ru(bpy)_3]^{2+}$, which binds to DNA in an electrostatic binding mode, has little effect on DNA viscosity. While EB, as a typical intercalator, increases the relative DNA viscosity for lengthening of the DNA double helix through intercalative binding. With increasing amount of **1** and **2**, the relative viscosities of CT-DNA increase steadily, similar to the case of EB. Increased DNA viscosity, which depends on the DNA-binding mode and affinity, follows the order of EB > **2** > **1** > $[Ru(bpy)_3]^{2+}$, suggesting that both complexes bind to DNA through intercalative binding, consistent with the above spectroscopic results.

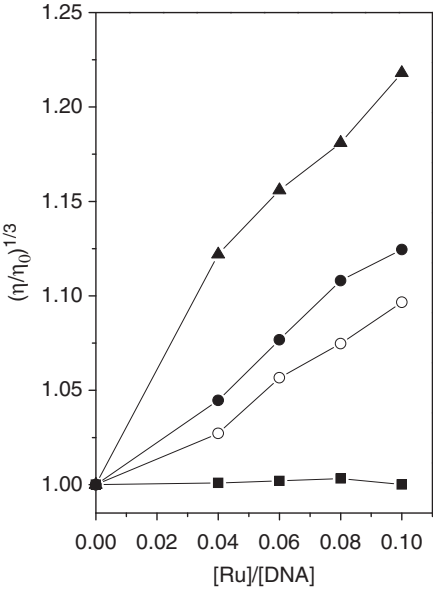

Figure 5. Effects of increase in amounts of EB (▲), **1** (○), **2** (●), and $[Ru(bpy)_3]^{2+}$ (■) on the relative viscosity of CT-DNA at 30 (±0.1)°C, respectively. The total concentration of DNA is 0.25 mmol L^{-1}.

3.6. *Photocleavage of pBR322 DNA by Ru(II) complexes*

Ru(II) complexes with polypyridyl ligands which cleave nucleic acids under irradiation are of interest due to their well-behaved redox and photochemical properties [56–58]. Upon irradiation, most generate singlet oxygen, thus inducing single-strand or double-strand cleavage of DNA [59]. The photocleavage behaviors of the two complexes on supercoiled pBR322 DNA were monitored by gel electrophoresis in TBE buffer (pH = 8.3). When circular plasmid DNA is subjected to gel electrophoresis, relatively fast migration will be observed for the intact supercoiled form (Form I). If scission occurs on one strand (nicked circulars), the supercoil form will relax to generate a slower moving nicked circular form (Form II). If both strands are cleaved, a linear form (Form III) that migrates between Forms I and II will be generated [58].

The abilities of **1** and **2** to induce photoactivated cleavage of pBR322 DNA upon irradiation at 365 nm were examined. As shown in figure 6, both complexes photocleave pBR322 DNA. No obvious DNA cleavage was observed for controls in the absence of the complexes (lane 0). On increasing the concentration of Ru(II) complexes, the amount of Form I of pBR322 DNA is decreased and that of Form II (nicked circular DNA) is increased. At 80 μmol L^{-1}, **2** almost promotes complete conversion of DNA from Form I to Form II. Thus **1** and **2** cleave DNA upon irradiation and **2** exhibits a higher efficiency in DNA-photocleavage than **1**. Compared to $[Ru(bpy)_2(dppz)]^{2+}$ [14, 23], **1** and **2** exhibit much higher DNA-photocleavage efficiency through modification of the dppz.

To establish the reactive species responsible for DNA photocleavage of **1** and **2**, the influence of different inhibitive agents was examined. Photoactivated cleavage of pBR322 DNA in the presence of **1** and **2** and different inhibitive agents are shown

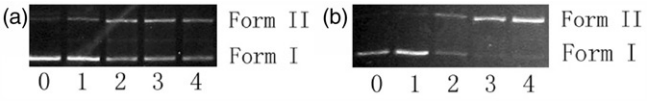

Figure 6. Photoactivated cleavage of pBR322 DNA in the presence of Ru(II) complexes after 2 h irradiation at 365 nm. Lane 0, DNA alone; Lanes 1–4: **1** (a) and **2** (b) at 10, 20, 40, and 80 μmol L^{-1}.

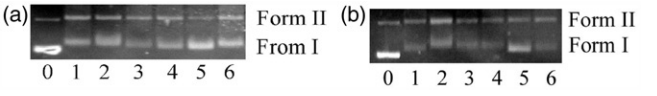

Figure 7. Agarose gel showing cleavage of pBR322 DNA incubated with **1** (a), **2** (b) and different inhibitors after 2 h irradiation at 365 nm, [Ru] = 80 μmol L^{-1}. Lane 0: DNA alone, Lane 1: DNA + Ru, Lanes 2–6: DNA + Ru + 1 μmol L^{-1} DMSO, 100 mmol L^{-1} mannitol, 1000 U·mL^{-1} SOD, 25 mmol L^{-1} NaN_3, 1.2 mmol L^{-1} histidine.

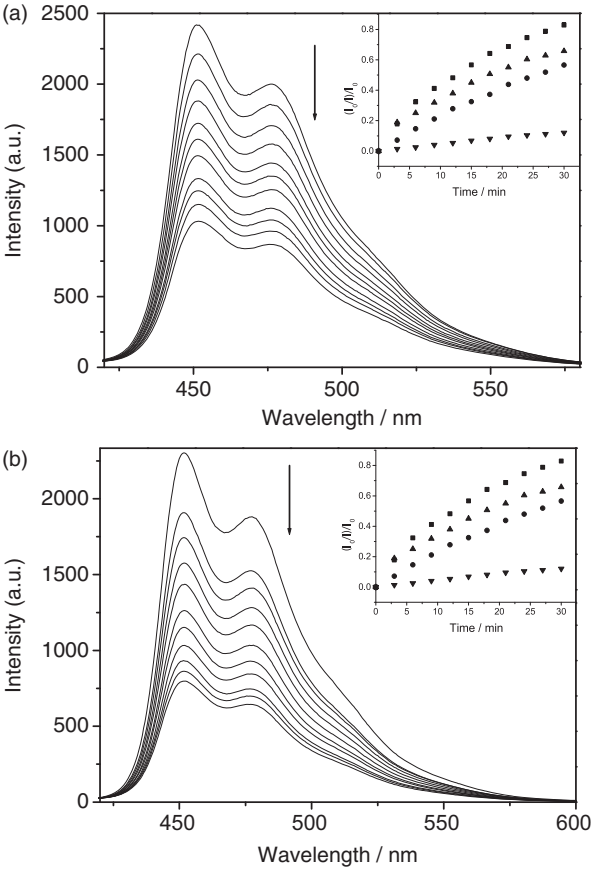

Figure 8. The emission spectral changes of DPBF in the presence of **1** (a) and **2** (b) upon irradiation at 450 nm. Inset: the DPBF consumption percentage as a function of irradiation time in air-equilibrated CH_3OH solution of $[Ru(bpy)_3]^{2+}$ (■), **1** (●), **2** (▲), and $[Ru(bpy)_2(dppz)]^{2+}$ (▼).

in figure 7. Singlet oxygen ($^1O_2$) scavengers [60], NaN_3, and histidine (lanes 5 and 6) efficiently inhibited the DNA-cleavage activity, suggesting that singlet oxygen ($^1O_2$) is likely the cleaving agent. However, hydroxyl radical ($OH^\bullet$) scavengers [36, 37, 61] (DMSO and mannitol) or superoxide anion radical ($O_2^{\bullet-}$) scavenger (SOD) did not inhibit DNA cleavage, indicating that superoxide anion radical ($O_2^{\bullet-}$) and hydroxyl radical ($OH^\bullet$) may not be the reactive species in the DNA cleavage of **1** and **2** under irradiation. The mechanism of DNA cleavage is an oxidative process by generating singlet oxygen.

To confirm the $^1O_2$ generation abilities of **1** and **2**, chemical trapping experiments were conducted to determine the $^1O_2$ generation quantum yield. Figure 8 shows emission spectra changes of DPBF in the presence of **1** and **2** upon irradiation at 450 nm. Using $[Ru(bpy)_3]^{2+}$ as standard ($\Phi_\Delta^s = 0.81$ [62]), the Φ_Δ of **1**, **2**, and $[Ru(bpy)_2(dppz)]^{2+}$ in CH_3OH were determined to be 0.63, 0.58, and 0.12, respectively. From figure 8, **1** and **2** are able to generate $^1O_2$ and produce much higher yield than $[Ru(bpy)_2(dppz)]^{2+}$, revealing that modification of the intercalating ligand dppz improves the $^1O_2$ generation abilities of the Ru(II)-dppz system.

4. Conclusion

A dppz-based ligand ipdp and its Ru(II) complexes $[Ru(bpy)_2(ipdp)]^{2+}$ **1** and $[Ru(phen)_2(ipdp)]^{2+}$ **2** have been synthesized and characterized. The DNA-binding and photocleavage properties of these two complexes have been investigated. Both complexes bind to DNA in an intercalative mode, and the DNA binding affinity of **2** is greater than **1**. Furthermore, the two complexes are efficient DNA-photocleavers upon irradiation at 365 nm, with **2** having stronger DNA-photocleavage efficiency than **1**. DNA cleavage by **1** and **2** is an oxidative process by generating singlet oxygen.

Acknowledgments

We are grateful to the support of the Doctoral Scientific Research Foundation of Hunan University of Arts and Science, the construct program of the key discipline in Hunan province (Applied Chemistry), the Scientific Research Foundation of Hunan Provincial Education Department (10C1002), and the Open Project Program of Key Laboratory of Environmentally Friendly Chemistry and Applications of Ministry of Education (10HJYH05).

References

[1] M.K. Nazeeruddin, C. Klein, P. Liska, M. Grätzel. *Coord. Chem. Rev.*, **249**, 1460 (2005).
[2] L.N. Ji, X.H. Zou, J.G. Liu. *Coord. Chem. Rev.*, **216–217**, 513 (2001).
[3] M.J. Clarke. *Coord. Chem. Rev.*, **236**, 209 (2003).
[4] J.C. Genereux, J.K. Barton. *Chem. Rev.*, **110**, 1642 (2010).
[5] A. Sassolas, B.D. Leca-Bouvier, L.J. Blum. *Chem. Rev.*, **108**, 109 (2008).
[6] H.K. Liu, P.J. Sadler. *Acc. Chem. Res.*, **44**, 349 (2011).
[7] Y. Liu, A. Chouai, N.N. Degtyareva, S.A. Lutterman, K.R. Dunbar, C. Turro. *J. Am. Chem. Soc.*, **127**, 10796 (2005).

[8] R.M. Hartshorn, J.K. Barton. *J. Am. Chem. Soc.*, **114**, 5919 (1992).
[9] Y.Z. Ma, H.J. Yin, K.Z. Wang. *J. Phys. Chem. B*, **113**, 11039 (2009).
[10] Y.J. Liu, C.H. Zeng, J.H. Yao, F.H. Wu, L.X. He, H.L. Huang. *Chem. Biodivers.*, **7**, 1770 (2010).
[11] L.F. Tan, F. Wang, H. Chao, Y.F. Zhou, C. Weng. *J. Inorg. Biochem.*, **101**, 700 (2007).
[12] Y.M. Chen, Y.J. Liu, Q. Li, K.Z. Wang. *J. Inorg. Biochem.*, **103**, 1395 (2009).
[13] Y.J. Liu, Z.H. Liang, Z.Z. Li, J.H. Yao, H.L. Huang. *J. Organomet. Chem.*, **696**, 2728 (2011).
[14] C. Sentage, J.C. Chambron, J.P. Sauvage, N. Pailous. *J. Photochem. Photobiol. B*, **26**, 165 (1994).
[15] S.P. Foxon, M.A.H. Alamiry, M.G. Walker, A.J.H.M. Meijer, I.V. Sazanovich, J.A. Weinstein, J.A. Thomas. *J. Phys. Chem. A*, **113**, 12754 (2009).
[16] C. Moucheron, A. Kirsch-De Mesmaeker, J.M. Kelly. *J. Photochem. Photobiol. B*, **40**, 91 (1997).
[17] S. Arounaguiri, B.G. Maiya. *Inorg. Chem.*, **38**, 842 (1999).
[18] A. Hergueta-Bravo, M.E. Jiménez-Hernández, F. Montero, E. Oliveros, G. Orellana. *J. Phys. Chem. B*, **106**, 4010 (2002).
[19] B. Elias, A. Kirsch-De Mesmaeker. *Coord. Chem. Rev.*, **250**, 1627 (2006).
[20] F. Gao, H. Chao, F. Zhou, Y.X. Yuan, B. Peng, L.N. Ji. *J. Inorg. Biochem.*, **100**, 1487 (2006).
[21] F. Gao, H. Chao, J.Q. Wang, Y.X. Yuan, B. Sun, Y.F. Wei, B. Peng, L.N. Ji. *J. Biol. Inorg. Chem.*, **12**, 1015 (2007).
[22] Y. Liu, R. Hammitt, D.A. Lutterman, R.P. Thummel, C. Turro. *Inorg. Chem.*, **46**, 6011 (2007).
[23] H.J. Yu, H. Chao, L. Jiang, L.Y. Li, S.M. Huang, L.N. Ji. *Inorg. Chem. Commun.*, **11**, 553 (2008).
[24] S.A. Tysoe, R. Kopelman, D. Schelzig. *Inorg. Chem.*, **38**, 5196 (1999).
[25] X.W. Liu, Y.M. Shen, J.L. Lu, Y.D. Chen, L. Li, D.S. Zhang. *Spectrochim. Acta, Part A*, **77**, 522 (2010).
[26] X.W. Liu, J.C. Chen, X. Hu, H. Li, K.C. Zheng, L.N. Ji. *Helv. Chim. Acta*, **91**, 1374 (2008).
[27] J.M. Lee, J.Y. Choi, J.M. Kim, S.Y. Lee, H. Lee, S.K. Kim, T.S. Cho. *Bull. Korean Chem. Soc.*, **28**, 965 (2007).
[28] Q.X. Zhen, B.H. Ye, J.G. Liu, Q.L. Zhang, L.N. Ji, L. Wang. *Inorg. Chim. Acta*, **303**, 141 (2000).
[29] X.W. Liu, L.C. Xu, H. Li, H. Chao, K.C. Zheng, L.N. Ji. *J. Mol. Struct.*, **920**, 163 (2009).
[30] P. Lincoln, A. Broo, B. Nordén. *J. Am. Chem. Soc.*, **118**, 2644 (1996).
[31] C. Moucheron, A.K.D. Mesmaeker, S. Choua. *Inorg. Chem.*, **36**, 584 (1997).
[32] M.K. Brennaman, T.J. Meyer, J.M. Papanikolas. *J. Phys. Chem. A*, **108**, 9938 (2004).
[33] L.M. Wilhelmsson, F. Westerlund, P. Lincoln, B. Nordén. *J. Am. Chem. Soc.*, **124**, 12092 (2002).
[34] B.P. Sullivan, D.J. Salmon, T.J. Meyer. *Inorg. Chem.*, **17**, 3334 (1978).
[35] F.E. Arnold. *J. Polym. Sci., Part A-1*, **8**, 2079 (1970).
[36] J. Bolger, A. Gourdon, E. Ishow, J.P. Launay. *Inorg. Chem.*, **35**, 2937 (1996).
[37] E. Ishow, A. Gourdon, J.P. Launay. *Chem. Commun.*, 1909 (1998).
[38] J.D. McGhee, P.H. von Hippel. *J. Mol. Biol.*, **86**, 469 (1974).
[39] A. Ambroise, B.G. Maiya. *Inorg. Chem.*, **39**, 4256 (2000).
[40] R.H. Young, K. Wehrly, R.L. Martin. *J. Am. Chem. Soc.*, **93**, 5774 (1971).
[41] H.Y. Ding, X.S. Wang, L.Q. Song, J.R. Chen, J.H. Yu, C. Li, B.W. Zhang. *J. Photochem. Photobiol., A*, **177**, 286 (2006).
[42] S. Ruhemann. *J. Chem. Soc.*, **97**, 1438 (1910).
[43] R. Shapiro, R. Chatterjie. *J. Org. Chem.*, **35**, 447 (1970).
[44] B.Y. Wu, L.H. Gao, Z.M. Duan, K.Z. Wang. *J. Inorg. Biochem.*, **99**, 1685 (2005).
[45] R.B. Nair, E.S. Teng, S.L. Kirkland, C.J. Murphy. *Inorg. Chem.*, **37**, 139 (1998).
[46] J.G. Liu, Q.L. Zhang, X.F. Shi, L.N. Ji. *Inorg. Chem.*, **40**, 5045 (2001).
[47] Y.J. Liu, X.Y. Guan, X.Y. Wei, L.X. He, W.J. Mei, J.H. Yao. *Transition Met. Chem.*, **33**, 289 (2011).
[48] C.V. Kumar, N.J. Turro, J.K. Barton. *J. Am. Chem. Soc.*, **107**, 5518 (1985).
[49] I. Ortmans, B. Elias, J.M. Kelly, C. Moucheron, A.K. Demesmaeker. *Dalton Trans.*, 668 (2004).
[50] M.J. Waring. *J. Mol. Biol.*, **13**, 269 (1965).
[51] J.B. LePecq, C. Paoletti. *J. Mol. Biol.*, **27**, 87 (1967).
[52] D.L. Boger, B.E. Fink, S.R. Brunette, W.C. Tse, M.P. Hedrick. *J. Am. Chem. Soc.*, **123**, 5878 (2001).
[53] S. Satyanarayana, J.C. Dabrowiak, J.B. Chaires. *Biochemistry*, **31**, 9319 (1992).
[54] S. Satyanarayana, J.C. Dabrowiak, J.B. Chaires. *Biochemistry*, **32**, 2573 (1993).
[55] M. Roy, B. Pathak, A.K. Patra, E.D. Jemmins, M. Nethaji, A.R. Chakravarty. *Inorg. Chem.*, **46**, 11112 (2007).
[56] Y.J. Sun, L.E. Joyce, N.M. Dickson, C. Turro. *Chem. Commun.*, **46**, 2426 (2010).
[57] G.J. Ryan, S. Quinn, T. Gunnlaugsson. *Inorg. Chem.*, **47**, 401 (2008).
[58] Q.X. Zhou, W.H. Lei, Y. Sun, J.R. Chen, C. Li, Y.J. Hou, X.S. Wang, B.W. Zhang. *Inorg. Chem.*, **49**, 4729 (2010).
[59] J.K. Barton, A.L. Raphael. *J. Am. Chem. Soc.*, **106**, 2466 (1984).
[60] F.R. Nilsson, P.B. Merkel, D.R. Kearns. *Photochem. Photobiol.*, **16**, 117 (1972).
[61] G. Cohen, H. Eisenberg. *Biopolymers*, **8**, 45 (1969).
[62] A.A. Abdel-Shafi, P.D. Beer, R.J. Mortimer, F. Wilkinson. *J. Phys. Chem. A*, **104**, 192 (2000).